HEFAT2014
10th International Conference on Heat Transfer, Fluid Mechanics and Thermodynamics
14 – 16 July 2014
Orlando, Florida

# SECOND LAW ANALYSIS OF THE FLOW OF TWO IMMISCIBLE COUPLE STRESS FLUIDS IN FOUR ZONES

Ramana Murthy J V[1,*], Srinivas J[1] and Sai K S[2]
[1]Department of Mathematics, National Institute of Technology, Warangal, 506004, India.
[2]Department of Mathematics, DMSSVH College of Engineering, Krishna-521002, India
*E-mail: jvrjosyula@yahoo.co.in

## ABSTRACT

This work investigates the entropy generation in a steady flow of two immiscible couple stress fluids in a horizontal channel bounded by two porous beds at the bottom and top. The flow is considered in FOUR zones: zone-IV contains the flow of viscous fluid in the large porous bed with low permeability at the bottom, zone-I and II contain free flow of two immiscible couple stress fluids and zone-III contains the flow of viscous fluid in the thin porous bed with high permeability at the top. The flow is assumed to be governed by Stokes's couple stress fluid flow equations in the free channel. In zone-IV, Darcy's law together with the Beavers-Joseph (B-J) slip condition at the interface is used whereas in zone-III Brinkman's model is used for flow. The plates of the channel are maintained at constant temperatures higher than that of the fluid. The closed form expressions for entropy generation number and Bejan number are derived in dimensionless form by using the expressions of velocity and temperature. The effects of relevant parameters on velocity, temperature, entropy generation number and Bejan number are analyzed and presented through graphs.

## INTRODUCTION

Contemporary engineering thermodynamics use a parameter called the rate of entropy generation (or production) to gauge the irreversibility's related to heat transfer, friction, and other non-idealities within systems. The second law of thermodynamics should be considered to evaluate the sources of irreversibility in flow and thermal systems. Conserving useful energy depends on designing efficient thermodynamic heat-transfer processes. Energy conversion processes are accompanied by an irreversible increase in entropy, which leads to a decrease in exergy (available energy). Thus, even though the energy is conserved, the quality of the available energy decreases because the energy is converted into a different form of energy, from which less work can be obtained. Reduced entropy generation results in more efficient designs of energy systems. Therefore, in recent years, the entropy minimization has become a topic of great interest in the thermo-fluid area. Bejan [1, 2, 3] focused on the different reasons behind the entropy generation in applied thermal engineering where the generation of entropy destroys the available work (exergy) of a system. Therefore, it makes good engineering sense to focus on the irreversibility of heat transfer and fluid flow processes, and try to understand the function of associated entropy generation mechanisms. Bejan [4] also carried out an extensive review on entropy generation minimization (EGM). The review traced the development and adoption of the method in several sectors of mainstream thermal engineering and science. Furthermore, many researchers carried out studies on the entropy generation in various flow cases. Bejan [1] studied the heat transfer problems in the pipe flow, boundary layer flow past a plate, and flow in the entrance region of a rectangular duct using EGM. He demonstrated that how the flow geometric parameters may be selected in order to minimize the irreversibility associated with a specific convective heat transfer.

There are many problems in the fields of hydrology and reservoir mechanics in which systems involving two or more immiscible fluids of different densities/viscosities flowing in same pipe or channel or through porous media are encountered. Typical fluid flow examples of these systems are: air-water, water-salt water, oil-water, gas-oil, and gas-oil -water systems. These are referred to as multi-phase flows in literature. Blood flow in arteries has been studied by many researchers considering blood as two phase flow. Several investigations on multi-phase flows are reported by various researchers such as Chaturani and Samy [5], Bird et al. [6], Ramchandra Rao and Srinivasan Usha [7], Bhattacharya [8], Kapur and Shukla [9] etc. The flow and heat transfer in immiscible fluids are of special importance in the petroleum extraction and transport problem. Heat transfer in immiscible flows were discussed by Bakhtiyarov and Siginer [10], Chamkha [11] etc.

Fluid flow in porous media is an important subject of widespread interest in hydrology, geophysics, biology and the petroleum industry. The problem of water coning is often encountered in the oil industry when a layer of water forms under a layer of oil. To understand this phenomenon, it is of interest to examine the contact layer at the flow of two immiscible fluids. So there has been widespread interest in the study of flow through channels and tubes in recent years. Vajravelu et al. [12] studied unsteady flow of two immiscible conducting fluids between two permeable beds. Vijayakumar and Syam Babu [13] discussed MHD viscous flow between two porous beds. Iyengar and Punnamchander [14] have studied the couple stress fluid flow between two porous beds.

Entropy generation calculations for different systems which have different geometries in porous or nonporous channels have been restricted to the first law of thermodynamics. Calculations using the second law of thermodynamics, which are related to entropy generation and efficiency calculation, are more reliable than first law-based calculations. A great volume of information is available dealing with second law analysis in

the flow field and heat transfer in a porous medium. Waqar and Gorla [15] have analyzed the second law characteristics of heat transfer and fluid flow due to mixed convection in non-Newtonian fluids over a horizontal plane. Hooman and Ejlali [16] studied both the first and the second laws of thermodynamics for thermally developing forced convection in a circular tube filled with a saturated porous medium. Tamayol et al. [17] studied thermal analysis of flow in a porous medium over a permeable stretching wall. Morosuk [18] discussed entropy generation in conduits filled with porous medium totally and partially. Mahmud and Fraser [19, 20] have discussed conjugate heat transfer inside a porous channel and magneto-hydrodynamic free convection and entropy generation in a square porous cavity and also mixed convection radiation interaction in a vertical porous channel. Tasnim et al. [21] studied entropy generation in a porous channel with hydro-magnetic effect. Kamel Hooman [22] discussed the second-law analysis of thermally developing forced convection in a porous medium. Chauhan and Vikas Kumar [23] described the effects of slip conditions on forced convection and entropy generation in a circular channel occupied by a highly porous medium governed by Darcy extended Brinkman-Forchheimer model. Paresh Vyas and Archana Rai [24] investigated the entropy generation in radiative MHD Couette flow of a Newtonian fluid in a parallel plate channel with a naturally permeable base. In recent years, the fluid flow and entropy generation in two immiscible fluids in a channel have received considerable attention by researchers. Kamisli and Oztop [25] considered the fluid flow and entropy generation in two immiscible fluids in a channel. These authors explained very nicely the thermodynamic interface conditions involved in a flow of immiscible fluids and made a significant observation that minimum temperature gradient in the transverse direction of the flow offers minimum entropy generation near the plates. Recently, Ramana Murthy and Srinivas [26] have studied the second law analysis for the flow of two immiscible micropolar fluids between two parallel plates. They observed that the entropy generation is more near the plates than at the interface of the channel.

*Couple stress fluids:* To the extent the present authors have surveyed the flow of immiscible incompressible couple stress fluids between two porous beds has not been studied so far. The consideration of couple-stress, in addition to the classical Cauchy stress, has led to the recent development of theories of fluid micro continua. This new branch of fluid mechanics has attracted a growing interest during recent years mainly because it possesses the mechanism to describe such rheologically complex fluids as liquid crystals, polymeric suspensions, and animal blood for which the Navier-Stoke's theory is inadequate. One such couple stress theory of fluids was developed by Stokes [27], and represents the simplest generalization of the classical theory which allows for polar effects such as the presence of couple stresses and body couples. The couple stress fluid is a special case of a non-Newtonian fluid which is intended to take into account the particle size effects. A review of couple stress (polar) fluid dynamics was reported by Stokes [28]. Ariman [29] discussed the applications on couple stress fluids and compared with that of micropolar fluids. A number of studies for such a fluid have been reported [30, 31].

The main objective of this paper is to study the entropy generation analysis for the flow of two immiscible couple stress fluids between two porous beds.

## PROBLEM FORMULATION AND GOVERNING EQUATIONS

Consider the flow of two immiscible couple stress fluids between two parallel plates distant 2h apart, bounded by two porous beds of different permeability's. The lower porous bed in zone-IV has low permeability with infinite thickness whereas the upper porous bed in zone-III is highly permeable with finite thickness H (Figure 1). The permeability's of lower and upper beds are $K_1$ and $K_2$ respectively. Let X and Y are the axial and vertical coordinates respectively with the origin at the centre of the channel. Fluid flow is generated due to a constant pressure gradient which acts at the mouth of the channel. The lower fluid (viscosity $\mu_1$, density $\rho_1$ and thermal conductivity $k_1$) occupies the region ($-h \le Y \le 0$) comprising the lower half of the channel and this region will be referred to as zone I. The upper fluid (viscosity $\mu_2$, density $\rho_2 (<\rho_1)$ and thermal conductivity $k_2$) is assumed to occupy the upper half of the channel (i.e., $0 \le Y \le h$), and this region is called zone II. The two walls of the channel are held at different temperatures $T_I$ and $T_{II}$ (with $T_I < T_{II}$). The equations for the flow in zone I and II (i.e., $-h \le Y \le h$) are assumed to be governed by couple stress fluid flow equations (neglecting body forces except gravity force and body couples) of Stokes [27, 28] and energy equation

$$\frac{d\rho}{dt} + \text{div}(\rho\bar{q}) = 0 \tag{1}$$

$$\rho\frac{d\bar{q}}{dt} = \frac{1}{2}\text{curl}(\rho\bar{l}) - \nabla P + \mu\,\text{curl}(\text{curl}\bar{q})) - \eta\,\text{curl}(\text{curl}(\text{curl}(\text{curl}\bar{q}))) + (\lambda+2\mu)\,\text{grad}(\text{div}\bar{q}) \tag{2}$$

$$\rho\frac{dE}{dt} = \Phi + k\nabla^2 T \tag{3}$$

$$\text{where } \Phi = \mu\left[(\text{grad}\bar{q}):(\text{grad}\bar{q})^T + (\text{grad}\bar{q}):(\text{grad}\bar{q})\right] + 4\eta\left[(\text{grad}\bar{\omega}):(\text{grad}\bar{\omega})^T\right] + 4\eta'\left[(\text{grad}\bar{\omega}):(\text{grad}\bar{\omega})\right]$$

The equations $(1)-(3)$ represent conservation of mass, balance of linear momentum and energy equation respectively. The scalar quantity $\rho$ is the density and $P$ is the fluid pressure at any point. The vectors $\bar{q}$, $\bar{\omega}$, $\bar{f}$ and $\bar{\ell}$ are the velocity, rotation, body force per unit mass and body couple per unit mass, respectively. The material constants $\lambda$ and $\mu$ are the viscosity coefficients and $\eta$ and $\eta'$ are the couple stress viscosity coefficients satisfying the constraints $\mu \ge 0$; $3\lambda+2\mu \ge 0$; $\eta \ge 0$, $|\eta'| \le \eta$. There is a length parameter $l = \sqrt{\eta/\mu}$ which is a characteristic measure of the polarity of the couple stress fluid and this parameter is identically zero in

the case of non-polar fluids. In the energy equation $\Phi$ is the dissipation function of mechanical energy per unit mass, $E$ is the specific internal energy, $\bar{\mathbf{h}} = -k\nabla T$ is the heat flux, where $k$ is the thermal conductivity and $T$ is the temperature.

The force stress tensor $t_{ij}$ and the couple stress tensor $M_{ij}$ that arises in the theory of couple stress fluids are given by

$$t_{ij}=\left(-P+\lambda div(\bar{q})\right)\delta_{ij}+2\mu d_{ij}+\frac{1}{2}\delta_{ijk}\left[m_{,k}+4\eta w_{k,rr}+\rho c_k\right] \quad (4)$$

$$M_{ij}=\frac{1}{3}m\delta_{ij}+4\eta\omega_{j,i}+4\eta'\omega_{j,i} \quad (5)$$

In the above $\bar{\omega}=\frac{1}{2}curl(\bar{q})$ is the spin vector, $\omega_{i,j}$ is the spin tensor and $\rho c_k$ is the body couple vector. $d_{ij}$ is the components of rate of shear strain, $\delta_{ij}$ is the Kronecker symbol, $\delta_{ijk}$ is the Levi-Civita symbol and comma denotes covariant differentiation.

Darcy's law is valid for the flows through porous bodies with low permeability. In applications where fluid velocities are low, such as movements of groundwater and petroleum, etc., Darcy's law well describes the fluid transport in porous media. Darcy law is the simplest and, by far, the most popular one, due to its simplicity. It states that the filtration velocity of the fluid is proportional to the difference between the body force and the pressure gradient. The constant K appearing in the relation is called the permeability of the medium. Since Darcy law is a first order PDE for the velocity, it cannot sustain the no-slip condition on an impermeable wall or a transmission condition of the contact with free flow. That motivated Brinkman to modify the Darcy law in order to be able to impose the no-slip boundary condition on an obstacle submerged in porous medium.

Certain flows that pass through bodies with high porosity do not follow the Darcy law. For this type of flows Beavers and Joseph [32] condition is not applicable. The Darcy law fails to describe the presence of an impermeable (solid) boundary. Brinkman model is applicable for this type of flows. Brinkman model is used in many applications as it allows one to resolve problems with boundary conditions on impermeable boundary as well as on the interface between porous medium and an open fluid domain. In this paper, Darcy law [33] for flow in zone IV and the Brinkman law [34] for flow in zone-III are taken.

The flow in the infinite porous bed (i.e. in zone IV) is governed by Darcy law

$$\bar{q}=\frac{K}{\mu}(\bar{f}-\nabla P)$$

The flow in the finite porous bed (i.e. in zone III) is governed by Brinkman equation

$$\nabla P=-\frac{\mu}{K}\bar{q}+\mu\nabla^2\bar{q}$$

The boundary conditions for the flow through porous beds need special attention. Generally the no-slip condition is valid on the boundary when a fluid flows past impermeable surfaces. But when it flows past permeable surfaces, the no-slip condition is no longer valid since there will be a migration of fluid, tangential to the boundary within the permeable surfaces. The velocity within the permeable beds will be different from the velocity of the fluid in the channel and we have to match the two velocities at the interface. Beavers and Joseph [32] based on their experimental investigations proposed that the slip velocity is related to the tangential stress (known as the Beavers and Joseph (BJ) condition).

$$\frac{dU}{dY}=\frac{\alpha^*}{\sqrt{K}}(U_S-Q) \quad (6)$$

Here Us is the slip velocity, i.e., the local averaged tangential velocity just outside the porous medium, Q is the velocity inside the porous bed, K is the permeability of the porous medium and the slip coefficient $\alpha^*$ is a dimensionless constant depending on the material properties of the interstices and the derivative $\frac{dU}{dY}$ is taking positive when the normal to the boundary into the fluid medium is in a positive direction. $\alpha^*$ varies from 0 to 5 for different porous material surfaces (Nield [35]).If $\alpha^*=0$, it indicates a perfect slip condition and $\alpha^*\to\infty$, we get no slip condition i.e., $U_s = Q$. When $K \to \infty$, the surface will be impermeable and the velocity of the fluid in the normal direction to the surface is zero.

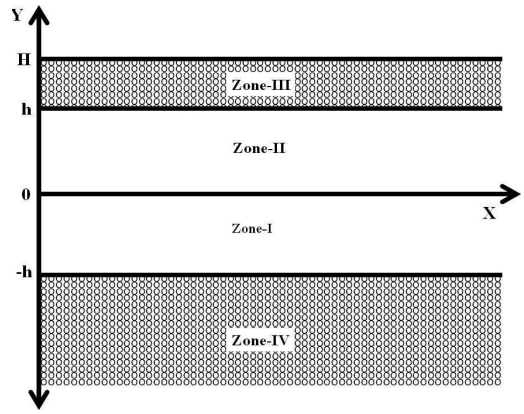


**Figure 1** Schematic of the investigated problem

Herein the velocity vector $\bar{q}$ is taken in the form $\bar{q}=(U(Y),0,0)$. Non-dimensional variables are introduced through: $x=\frac{X}{h}$, $y=\frac{Y}{h}$, $u=\frac{U}{U_o}$ and $p=\frac{P}{\rho_1 U_o^2}$ where $U_o$ is the maximum velocity of the fluid in the channel.

Neglecting body forces and body couples from the equation (2), we get the following set of non-dimensional form of governing equations and boundary conditions corresponding to the flow in two zones.

The governing equations in the corresponding zones are:

Zone I:$(-1 \le y \le 0)$

$$\frac{d^4u_1}{dy^4} - s_1 \frac{d^2u_1}{dy^2} = - \mathrm{Re}\, s_1 \frac{dp}{dx} \quad (7)$$

Zone II:$(0 \le y \le 1)$

$$\frac{d^4u_2}{dy^4} - s_2 \frac{d^2u_2}{dy^2} = - \mathrm{Re}\, s_2 \frac{n_\rho}{n_\mu} \frac{dp}{dx} \quad (8)$$

Zone III:$(1 \le y \le (1+\delta))$

$$\frac{d^3u_3}{dy^3} - \frac{1}{\mathrm{Da}\, n_k} u_3 = \mathrm{Re} \frac{n_\rho}{n_\mu} \frac{dp}{dx} \quad (9)$$

Zone IV:$(y \le -1)$

$$u_4 = -\mathrm{Da}\, \mathrm{Re} \frac{dp}{dx} \quad (10)$$

where $\mathrm{Re}=\frac{\rho_1 U_o h}{\mu_1}$ is the Reynolds number, $\mathrm{Da}=\frac{K_1}{h^2}$ is the Darcy number, $n_\mu=\frac{\mu_2}{\mu_1}$ is the viscosity ratio, $n_\rho=\frac{\rho_2}{\rho_1}$ is the density ratio, $n_K=\frac{K_2}{K_1}$ is the permeability ratio, $s_i=\frac{\kappa_i h^2}{\gamma}$ is the couple stress parameter, (i=1,2) and $\delta=\frac{H}{h}$.

**Boundary and interface conditions:**

A characteristic feature of the two-layer flow problem is the coupling across liquid-liquid interfaces. The liquid layers are mechanically coupled via transfer of momentum across the interfaces. Transfer of momentum results from the continuity of tangential velocity and a stress balance across the interface.

V. K. Stokes has proposed two types of boundary conditions (A) and (B) respectively and the vanishing of couple stresses on the boundary is referred to as condition (A) [28]. This condition is adopted here as this is appropriate in the present context.

At the lower porous boundary, couple stress vanishes: Beavers-Joseph (BJ) slip condition is taken at the lower porous bed i.e.,

$$\frac{du}{dy} = \frac{\alpha^* h}{\sqrt{K_1}} (u_s - u_p) \text{ where } u_p = -\mathrm{Da}\, \mathrm{Re} \frac{dp}{dx} \quad (11)$$

$$u(-1)=u_s \quad \text{and} \quad \frac{d^2u_1}{dy^2}=0 \text{ (condition(A))} \quad \text{at} \quad y=-1 \quad (12)$$

At the fluid interface velocity, vorticity, shear stress and couple stress are continuous:

$$u_{1(0^=)} = u_{2(0^+)},$$

$$\left.\frac{du_1}{dy}\right|_{(0^-)} = \left.\frac{du_2}{dy}\right|_{(0^+)}, \left(s_1 \frac{du_1}{dy} - \frac{d^3u_1}{dy^3}\right)_{(0^-)} = n_\eta \left(s_2 \frac{du_2}{dy} - \frac{d^3u_2}{dy^3}\right)_{(0^+)}$$

$$\text{and} \left(\frac{d^2u_1}{dy^2}\right)_{(0^-)} = n_\eta \left(\frac{d^2u_2}{dy^2}\right)_{(0^+)} \quad (13)$$

Where $n_\eta = \frac{\eta_2}{\eta_1}$ is the couple stress coefficient ratio.

At the upper plate boundary, velocity and shear stress are continuous and couple stresses vanish due to no slip and hyper-stick conditions:

$$u_{2(1^=)} = u_{3(1^+)}, \left(s_2 \frac{du_2}{dy} - \frac{d^3u_2}{dy^3}\right)_{(1^-)} = \left(s_2 \frac{du_3}{dy}\right)_{(1^+)} \text{ and}$$

$$\frac{d^2u_2}{dy^2} = 0 \text{(condition (A)) at } y = 1 \quad (14)$$

No slip condition: $u_3=0$ at $y=1+\delta$ (15)

where $u_s$ and $u_p$ are respectively the dimensionless slip velocity and Darcy's velocity.

## SOLUTION OF THE PROBLEM

**Velocity distributions:**

Solving equations (7) and (10), we see that the velocity components in the zones as:

Zone I: $(-1 \le y \le 0)$

$$u_1(y) = c_{11} + c_{12}y + c_{13}\cosh s_1 y + c_{14}\sinh s_1 y + \frac{1}{2}\mathrm{Re}\, B y^2 \quad (16)$$

Zone II: $(0 \le y \le 1)$

$$u_2(y) = c_{21} + c_{22}y + c_{23}\cosh s_2 y + c_{24}\sinh s_2 y + \frac{1}{2}\frac{n_\rho}{n_\mu}\mathrm{Re}\, B y^2 \quad (17)$$

Zone III: $(1 \le y \le 1+\delta)$

$$u_3(y) = c_{31}\cosh\left[\frac{1}{\sqrt{\mathrm{Da}\, n_K}}\right] y + c_{32}\sinh\left[\frac{1}{\sqrt{\mathrm{Da}\, n_K}}\right] y - \frac{n_\rho}{n_\mu}\mathrm{Da}\, n_K\, \mathrm{Re} B \quad (18)$$

Zone IV: $(y \le -1)$

$$u_4(y) = -\mathrm{Da}\, \mathrm{Re}\, B \quad (19)$$

where $B = \frac{dp}{dx}$ (constant). Here we take the solutions as: zone I: $u = u_1(y)$, zone II: $u = u_2(y)$, zone III: $u = u_3(y)$ and zone IV: $u = u_4(y)$. These involve 11 constants $c_{11}$, $c_{12}$, $c_{13}$, $c_{14}$, $c_{21}$, $c_{22}$,$c_{23}$, $c_{24}$, $c_{31}$, $c_{32}$ and $u_s$. These constants are found from the 11 boundary conditions given in (11) - (15) and these are obtained using Mathematica. As the expressions are cumbersome and they are not presented here.

**Heat transfer analysis:**

Once the velocity distributions are known, the temperature distributions for the two zones are determined by solving the energy equation (3) in the respective zones, subject to the appropriate boundary and interface conditions. Thermal coupling is achieved through continuity of temperature at the interface and the balance of heat flux across the interface. In the present problem, it is assumed that the two walls are maintained at constant temperatures $T_I$ and $T_{II}$ ($T_I < T_{II}$).

The governing equation for the temperature $T_I$ of the conducting fluid in zone I is then given by

$$k_1 \frac{d^2T_1}{dY^2} = -\left[\mu_1\left(\frac{dU_1}{dY}\right)^2 + \eta_1\left(\frac{d^2U_1}{dY^2}\right)^2\right] = 0 \qquad (20)$$

The governing equation for the temperature TII of the conducting fluid in zone II is then given by

$$k_2 \frac{d^2T_2}{dY^2} = -\left[\mu_2\left(\frac{dU_2}{dY}\right)^2 + \eta_2\left(\frac{d^2U_2}{dY^2}\right)^2\right] = 0 \qquad (21)$$

In order to non-dimensionalize the above equations (20)-(21), the following transformation is used for non-dimensional temperature θ: $\theta = \dfrac{T - T_I}{T_{II} - T_I}$.

The equations (20) and (21) are then reduced to the following form:

$$\frac{d^2\theta_1}{dy^2} + Br\left[\left(\frac{du_1}{dy}\right)^2 + \frac{1}{s_1}\left(\frac{d^2u_1}{dy^2}\right)^2\right] = 0 \qquad (22)$$

$$\frac{d^2\theta_2}{dy^2} + \frac{Br\, n_\mu}{n_k}\left[\left(\frac{du_2}{dy}\right)^2 + \frac{1}{s_2}\left(\frac{d^2u_2}{dy^2}\right)^2\right] = 0 \qquad (23)$$

where Br = Ek Pr is the Brinkman number, $Pr = \dfrac{\mu_1 c_{p1}}{k_1}$ is the Prandtl number, $Ek = \dfrac{U_o^2}{c_{p1}(T_{II} - T_I)}$ is the Eckert number and $n_k = \dfrac{k_2}{k_1}$ is the thermal conductivity ratio.

In the non-dimensional form, the boundary conditions for temperature and heat flux at the walls and interface become:

(i) at the lower and upper plate boundaries the temperatures are respectively,

$$\theta_1(y) = 0 \text{ and } y = -1 \text{ and } \theta_2(y) = 1 \text{ at } y = 1 \qquad (24)$$

(ii) at the fluid interface temperature (θ) and heat flux ($\bar{h}$) are continuous:

$$\theta_1(y) = \theta_2(y) \text{ and } \frac{d\theta_1}{dy} = n_k \frac{d\theta_2}{dy} \text{ at } y=0 \qquad (25)$$

The solutions of equations (22) and (23) with boundary and interface conditions are solved analytically and they are lengthy not shown here. The solution involves 4 constants $c_{15}$, $c_{16}$, $c_{25}$ and $c_{26}$ and these are found from the 4 boundary conditions (equations (24) and (25)) and are obtained using Mathematica.

## ENTROPY GENERATION ANALYSIS

Once the velocity and temperature fields have been obtained, one can determine the entropy generation distribution in a flow channel. This function, which characterizes the irreversible behavior of system, will be used to optimize (minimize) the entropy generation rate by evaluating parameters as well as fluid properties.

The convection process in a channel is inherently irreversible. Non-equilibrium conditions arise due to the exchange of energy and momentum within the fluid and at the solid boundaries. This causes the continuous entropy generation. One portion of this entropy production is due to heat transfer in the direction of finite temperature gradients. Another portion of the entropy production arises due to fluid friction irreversibility. The volumetric rate of entropy generation for incompressible couple stress fluid is given as follows

$$(S_i)_G = \frac{k}{T_o^2}(\nabla T)^2 + \frac{1}{T_o}\Phi$$

where Φ is the viscous dissipation function.

The volumetric rate of entropy generation reduces to

$$(S_i)_G = \frac{k_i}{T_o^2}\left(\frac{\partial T_i}{\partial Y}\right)^2 + \frac{\mu_i}{T_o}\left(\frac{\partial U_i}{\partial Y}\right)^2 + \frac{\eta_i}{T_o}\left(\frac{\partial^2 U_i}{\partial Y^2}\right)^2 \qquad (26)$$

where the value of i can be either 1 or 2 that represents fluid I or fluid II, respectively. On the right hand side of the above equation, the first term is the entropy generation due to heat conduction and the remaining two terms represent the entropy generation due to the viscous dissipation function Φ for an incompressible couple stress fluid.

The characteristic entropy generation rate $S_{G,C}$ is defined as,

$$S_{G,C} = \left[\frac{(\bar{h}_I)^2}{k_1 T_o^2}\right] = \left[\frac{k_1(\Delta T)^2}{h^2 T_o^2}\right] \qquad (27)$$

In the above equation, $\bar{h}_I$ is the heat flux in zone I, $T_o$ is the average, characteristic, absolute reference temperature of the medium, $\Delta T = T_{II} - T_I$ and h is the half of transverse distance of the channel.

The dimensionless form of entropy generation is the entropy generation number (Ns) is the ratio of the volumetric entropy generation rate $(S_i)_G$ to a characteristics transfer rate $S_{G,C}$.

$$Ns_i = \frac{(S_i)_G}{S_{G,C}} \text{ (i=1,2)}$$

The entropy generation number for each fluid with dimensionless variables are given by

$$Ns_1 = \left(\frac{d\theta_1}{dy}\right)^2 + \left(\frac{Br}{\Omega}\right)\left[\left(\frac{du_1}{dy}\right)^2 + \frac{1}{s_1}\left(\frac{d^2u_1}{dy^2}\right)^2\right] \quad (28)$$

$$Ns_2 = n_k\left(\frac{d\theta_2}{dy}\right)^2 + \left(\frac{Br}{\Omega}\right)n_\mu\left[\left(\frac{du_2}{dy}\right)^2 + \frac{1}{s_2}\left(\frac{d^2u_2}{dy^2}\right)^2\right] \quad (29)$$

where $Br=\left(\frac{\mu_1 U_o^2}{k_1\Delta T}\right)$ is the Brinkman number, which determines the importance of viscous dissipation because of the fluid frictions relative to the conduction heat flow resulting from the impressed temperature difference and $\Omega = \left(\Delta T/T_o\right)$ is the dimensionless temperature difference.

It is desirable to consider the Ek and Pr in a group that is called the Brinkman number (Br = Ek.Pr) for evaluating the relative importance of the energy due to viscous dissipation to the energy because of heat conduction. It was reported that Br is much less than unity for many engineering processes [1].

Entropy generates in a process or system due to the presence of irreversibility [3, 36]. In convective problem both fluid friction and heat transfer have contributions to the rate of entropy generation. Expression of the entropy generation number (Ns) is good for generating entropy generation profiles but fails to give any idea about the relative importance of friction and heat transfer effects. The domination of the irreversibility mechanisms is physically important since the entropy generation number is unable to overcome this problem. Two alternate parameters, irreversibility distribution ratio ($\phi$) and Bejan number (Be), are introduced for this purpose and they are gaining an increasing popularity among researchers studying the second law.

The idea of irreversibility distribution ratio $\phi$ can enhance the understanding of the irreversibility's associated with the heat transfer and the fluid friction. It is defined as the ratio of entropy generation due to fluid frictions (Nf) to heat transfer in the transverse direction (Ny) i.e.,

$$\phi = \frac{S_{G,\text{fluid friction}}}{S_{G,\text{heat transfer}}} = \left(\frac{Nf}{Ny}\right) \quad (30)$$

$\phi$ can be interpreted as follows: If $0 \le \phi < 1$, then $\phi$ indicates that heat transfer irreversibility dominates and if $\phi > 1$ the fluid friction dominates. For the case of $\phi = 1$, both the heat transfer and fluid friction have the same contribution for entropy generation.

An alternative irreversibility distribution parameter, called Bejan number Be, was defined by Paoletti et al., [37] as ratio of entropy generation due to heat transfer to the total entropy generation and it is given by

$$Be = \frac{Ny}{Ns} = \frac{Ny}{Ny + Nf} = \frac{1}{1+\varphi} \quad (31)$$

This is employed to understand the entropy generation mechanisms in thermal systems. Clearly, the value of the Bejan number ranges from 0 to 1. For Be>0.5, the entropy generation due to the heat transfer dominates, and this corresponds to the case of $\phi \to 0$. On the other hand, Be<0.5 refers to the entropy generation effects due to the fluid friction. This corresponds to $\phi \to 1$. When Be=0.5, the contributions of the heat transfer and fluid friction in the entropy generation are equal, and this corresponds to the case of $\phi = 1$.

## RESULTS AND DISCUSSION

The closed form solutions for the flow of two immiscible couple stress fluids between two porous beds are obtained and reported in the previous section. Numerical work is undertaken and the variations of velocity, temperature, entropy generation rate and Bejan number for different values of parameters are shown through figures.

**Flow Field:**

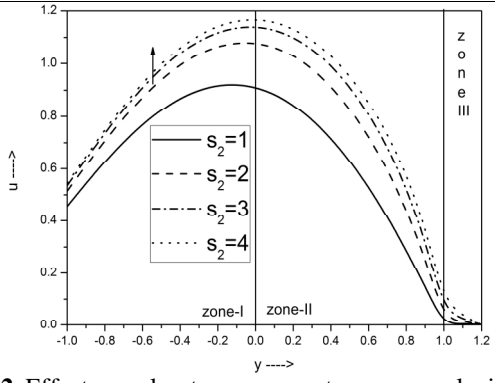


**Figure 2** Effect couple stress parameter $s_2$ on velocity u for $\delta$=0.2, $\alpha^*$=0.6, B=-0.8, Da=0.08, $n_\rho$=0.9, $n_\eta$=0.9, $n_K$=1.2, $n_\mu$=0.9, Re=2, $s_1$=1.5.

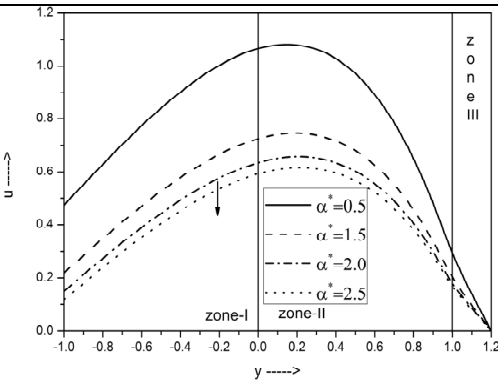


**Figure 3** Effect of slip parameter $\alpha^*$ on velocity u for $\delta$=0.2, B=-0.2, Da=0.08, $n_\rho$=0.9, $n_\eta$=0.9, $n_K$=1.2, $n_\mu$=0.9, Re=2, $s_2$=1.2, $s_1$=1.2.

The influence of the couple stress parameter $s_2$ on the velocity field is shown in Figure 2. It is seen that as $s_2$ increases, the velocity increases. As $s_2 \to \infty$ we get the case of Newtonian fluid. It can be concluded that the velocity of viscous fluid is more than that of couple stress fluid. Thus, the presence of couple stresses in the fluid increases the velocity. Figure 3 depicts the effects of the slip parameter $\alpha^*$ on the velocity field. As $\alpha^*$ increases, the velocity decreases. This change in velocity is seen to be more near the lower porous bed where Darcy law is applicable. The effect of the Darcy number

Da on the velocity field is shown in Figure 4. It is seen that as Da increases, the velocity increases in all regions of the channel.

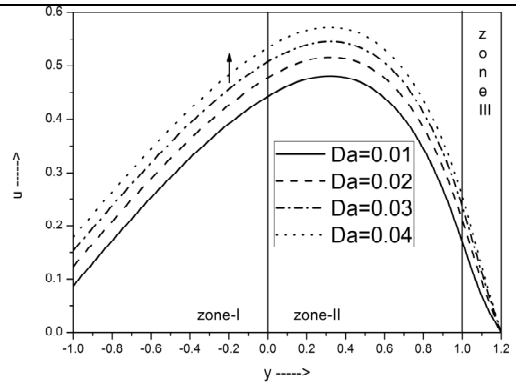


**Figure 4** Effect of Darcy number Da on velocity u for $\delta$=0.2, $\alpha^*$=0.5, B=-0.1, $n_\rho$=0.8, $n_\eta$=0.8, $n_K$=1.2, $n_\mu$=0.9, Re=2, $s_2$=2, $s_1$=2.

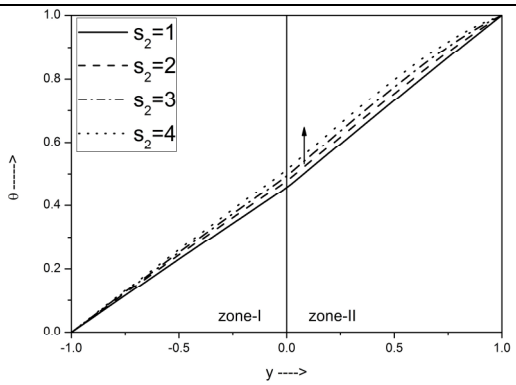


**Figure 5** Effect of couple stress parameter $s_2$ on temperature $\theta$ for $\delta$=0.2, $\alpha^*$=0.5, B=-0.9, Br=0.1, Da=0.02, $n_\rho$=0.9, $n_\eta$=0.9, $n_k$=0.9, $n_K$=1.2, $n_\mu$=0.9, Re=2, $s_1$=2.

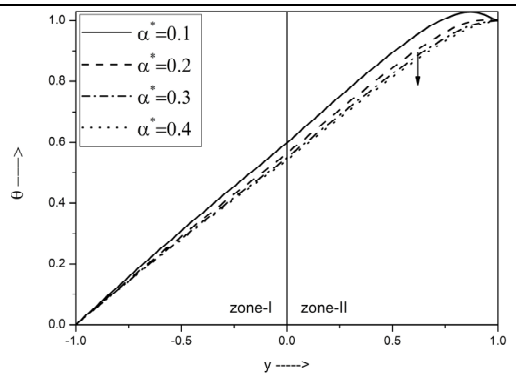


**Figure 6** Effect of slip parameter $\alpha^*$ on temperature $\theta$ for $\delta$=0.2, B=-0.3, Br=0.1, Da=0.08, $n_\rho$=0.9, $n_\eta$=0.7, $n_k$=0.9, $n_K$=1.2, $n_\mu$=0.9, Re=2, $s_1$=3, $s_2$=3.

**Thermal field and Heat transfer:**

Figure 5 displays the effect of the couple stress parameter $s_2$ on the temperature field. As the couple stress parameter $s_2$ increases, the temperature increases. Figure 6 presents the effects of slip parameter $\alpha^*$on the temperature distribution. As the slip parameter $\alpha^*$ increases, temperature decreases. The effect of an increase in Darcy parameter Da on temperature field is found to increase it in both zones of the channel as shown in Figure 7. Figure 8 indicates that the temperature increases with increasing the Brinkman number Br. This may be due to viscous dissipation.

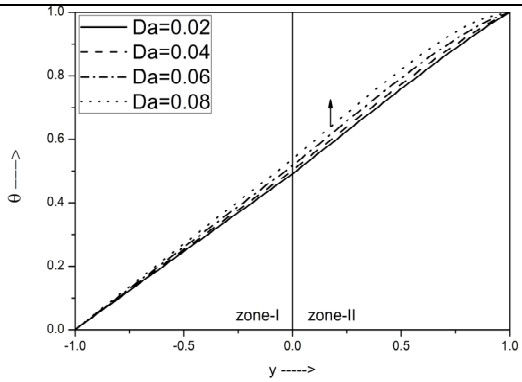


**Figure 7** Effect of Darcy number Da on temperature $\theta$ for $\delta$=0.2, $\alpha^*$=0.1, B=-0.1, Br=0.1, $n_\rho$=0.9, $n_\eta$=0.8, $n_k$=0.9, $n_K$=1.2, $n_\mu$=0.8, Re=1.2, $s_1$=2, $s_2$=2.

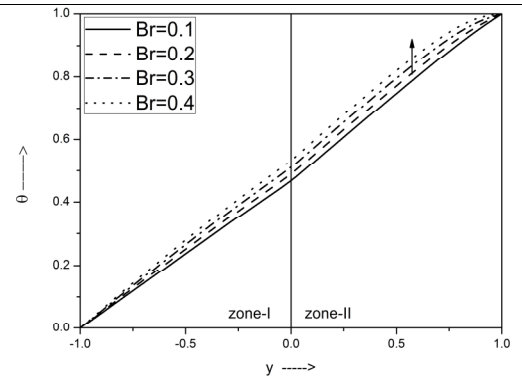


**Figure 8** Effect of Brinkman number Br on temperature $\theta$ for $\delta$=0.2, $\alpha^*$=0.8, B=-0.3, Da=0.08, $n_\rho$=0.8, $n_\eta$=0.8, $n_k$=0.8, $n_K$=0.8, $n_\mu$=0.8, Re=1.2, $s_1$=3, $s_2$=3.

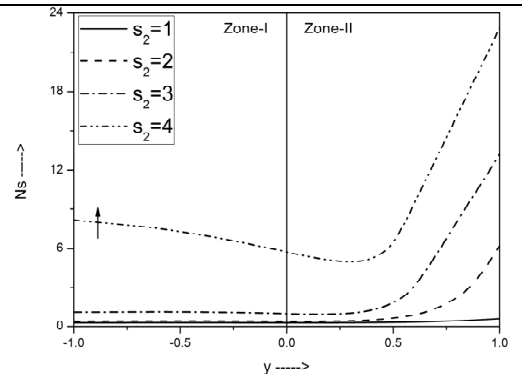


**Figure 9** Effect of couple stress parameter $s_2$ on Entropy generation number Ns for $\delta$=0.2, $\alpha^*$=2, B=-0.1, Br=1.5, Da=0.01, $n_\rho$=0.9, $n_\eta$=0.9, $n_k$=1, $n_K$=0.9, $n_\mu$=0.9, Re=5, $s_1$=5, $\Omega$=1.

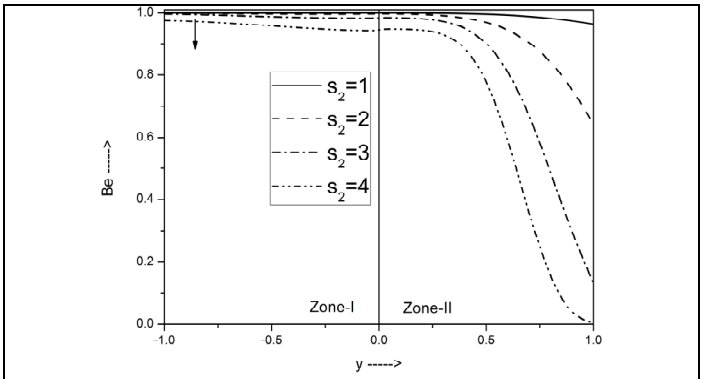


**Figure 10** Effect of couple stress parameter $s_2$ on Bejan number Be for δ=0.2, α*=2, B=-0.1, Br=0.2, Da=0.01, $n_\rho$=0.9, $n_\eta$=0.9, $n_k$=1, $n_K$=1.2, $n_\mu$=0.9, Re=2.2, $s_1$=5, Ω=1.

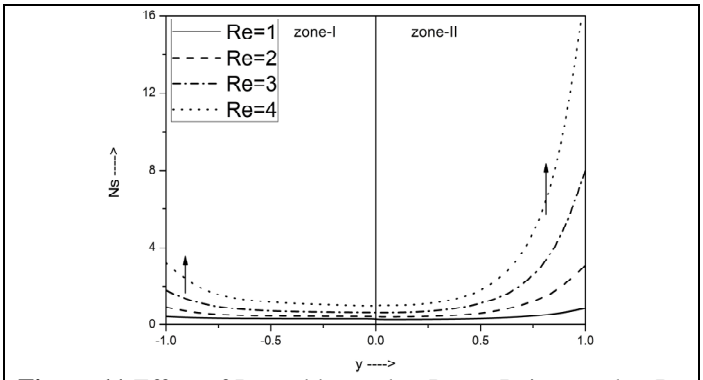


**Figure 11** Effect of Reynolds number Re on Bejan number Be for δ=0.2, α*=0.1, B=-0.8, Br=0.1, Da=0.01, $n_\rho$=0.9, $n_\eta$=0.9, $n_k$=1, $n_K$=0.9, $n_\mu$=0.9, $s_1$=5, $s_2$=5, Ω=1.

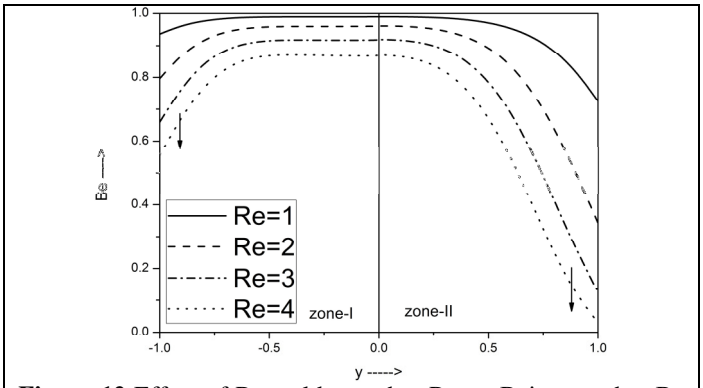


**Figure 12** Effect of Reynolds number Re on Bejan number Be for δ=0.2, α*=0.1, B=-0.1, Br=0.9, Da=0.01, $n_\rho$=0.6, $n_\eta$=0.6, $n_k$=0.8, $n_K$=0.8, $n_\mu$=0.9, $s_1$=2.5, $s_2$=2.5, Ω=1.

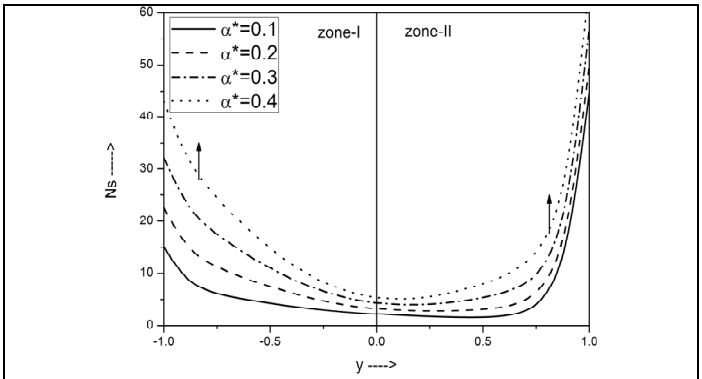


**Figure 13** Effect of slip parameter α* on Entropy generation number Ns for δ=0.2, B=-0.5, Br=0.1, Da=0.01, $n_\rho$=0.6, $n_\eta$=0.6, $n_k$=1, $n_K$=1.2, $n_\mu$=0.9, Re=2, $s_1$=2, $s_2$=2,Ω=1.

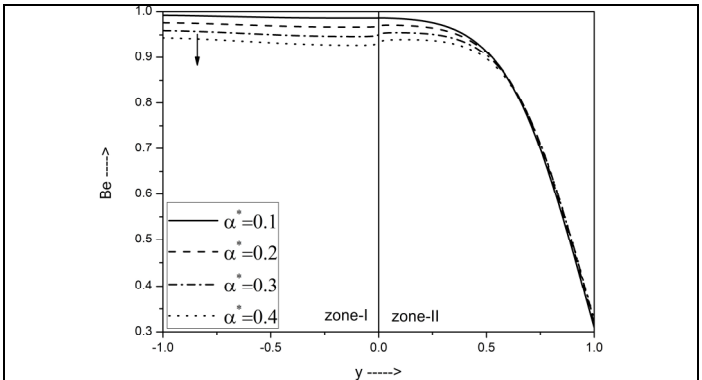


**Figure 14** Effect of slip parameter α* on Bejan number Be for δ=0.2, B=-0.5, Br=0.1, Da=0.01, $n_\rho$=0.6, $n_\eta$=0.6, $n_k$=1, $n_K$=1.2, $n_\mu$=0.9, Re=2,$s_1$=2, $s_2$=2,Ω=1.

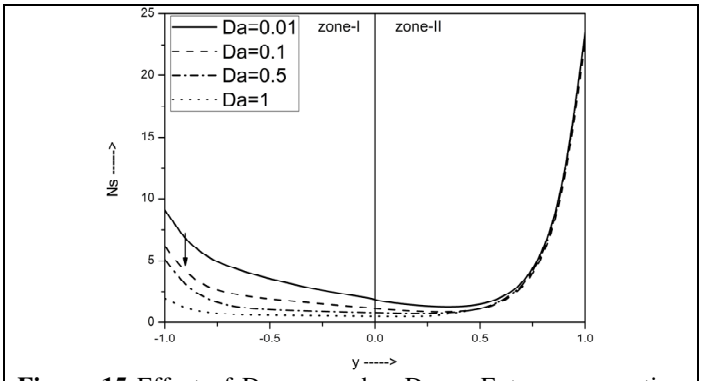


**Figure 15** Effect of Darcy number Da on Entropy generation number Ns for δ=0.2, α*=0.8, B=-0.5, Br=0.1, $n_\rho$=0.6, $n_\eta$=0.6, $n_k$=1, $n_K$=0.8, $n_\mu$=0.9, Re=3, $s_1$=3, $s_2$=3,Ω=1.

**Entropy generation and Heat transfer irreversibility:**

Figure 9 demonstrates the effect of couple stress parameter $s_2$ on the entropy generation number Ns. As the couple stress parameter increases, the entropy generation near the plates increases more rapidly in the fluid for the corresponding parameter. Ns is more on values near the plates in zone-I, than in the zone-II. This may be due to the more viscous nature of the fluid in zone-I.

Figure 10 illustrates the effect of couple stress parameter $s_2$ on Bejan number Be. As $s_2$ increases Bejan number decreases. A slight increase in couple stress parameter $s_2$, increases Bejan number Be huge at the interface and is nearly zero near the plates. Hence we conclude that near the plates the entropy generation rate due to conduction in the transverse direction is almost zero and entire entropy generation rate is due to fluid frictions only. From the limiting case of $s_2 \to \infty$, we

see that for viscous fluids, values of Be are less than the values of Be in couple stress fluids. With this we conclude that energy dissipation is more for viscous fluids than for couple stress fluids.

Figure 11 shows the effect of Reynolds number Re on the entropy generation number Ns. The entropy generation near the plates increases more rapidly in the fluid I than in the fluid II. This is due to the fact that in zone-I fluid is more viscous. Figure 12 shows the effect of Reynolds number Re on Bejan number Be. As Re increases, Be decreases. The variation of Be near the plates is more than the variation at the interface.

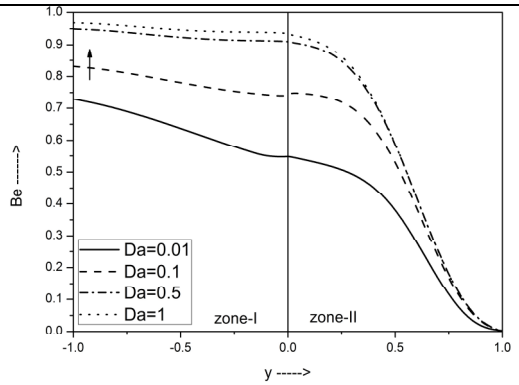


**Figure 16** Effect of Darcy number Da on Bejan number Be for $\delta$=0.2, $\alpha^*$=0.5, B=-0.2, Br=0.2, $n_\rho$=0.6, $n_\eta$=0.6, $n_k$=1, $n_K$=1.2, $n_\mu$=0.9, Re=2, $s_1$=2.5, $s_2$=2.5, $\Omega$=1.

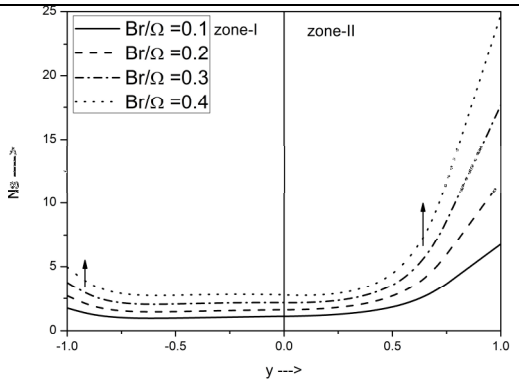


**Figure 17** Effect of dissipation parameter (Br/$\Omega$) on Entropy generation number Ns for $\delta$=0.2, $\alpha^*$=0.1, B=-0.1, Da=0.01, $n_\rho$=0.6, $n_\eta$=0.6, $n_k$=1, $n_K$=0.8, $n_\mu$=0.9, Re=2, $s_1$=3, $s_2$=3.

Figure 13 predicts the entropy generation for different values of slip parameter $\alpha^*$. As the slip parameter $\alpha^*$is increasing, the entropy generation is increasing in zone-I only where the slip condition is applied. $\alpha^* \to \infty$ indicates no-slip condition, velocity decreases as $\alpha^*$ increases. The same is observed in Figure 3. Hence when friction increases, entropy generation rate increases. Figure 14 describes the Bejan number Be profiles for different values of slip parameter. As the slip parameter $\alpha^*$ increases, the Bejan number decreases. This is in good agreement with the previous observation in Figure 13 for entropy generation rate.

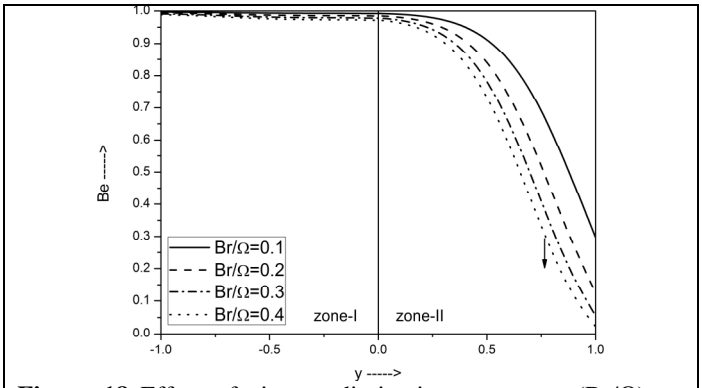


**Figure 18** Effect of viscous dissipation parameter (Br/$\Omega$) on Bejan number Be for $\delta$=0.2, $\alpha^*$=2, B=-0.1, Da=0.01, $n_\rho$=0.6, $n_\eta$=0.6, $n_k$=0.8, $n_K$=0.8, $n_\mu$=0.9, Re=2, $s_1$=2.5, $s_2$=2.5.

Figure 15 demonstrates the entropy generation for different values of Darcy number Da. As the Darcy number Da is increasing, the entropy generation is decreasing. Figure 16 describes the Bejan number Be profiles for different values of Darcy number Da. As the Darcy number Da is increasing, the Bejan number is increasing.

From Figure 17, we observe that as the viscous dissipation parameter (Br/$\Omega$) increases, entropy generation number Ns increases. The more the viscosity of the fluid is, the more is the entropy generation. It is observed that Ns $\cong$ 0 at the interface of the channel. This implies that at the interface, entropy generation is minimum (almost zero) i.e., exergy (available energy) is maximum and hence at the interface almost dissipation of energy is zero. From Figure 18, we observe that the Bejan number is maximum at the interface of the channel and decreases as we move towards the channel walls in either direction. The Bejan number decreases as the viscous dissipation parameter (Br/$\Omega$) increases.

## CONCLUSIONS

The first and second laws (of thermodynamics) aspects of fluid flow and heat transfer in a channel of two immiscible couple stress fluids between two porous beds is investigated analytically. The velocity and temperature profiles are found analytically. The exergy loss distribution is studied in terms of the second law of thermodynamics. The effect of viscous dissipation parameter (Br/$\Omega$) on the entropy generation number (Ns) and Bejan number (Be) are studied analytically. The computational results are presented through figures. The following observations are made from the above analysis:

1. The presence of couple stresses in the fluid increases the velocity and temperature.
2. Viscous dissipation parameter has a significant effect on the entropy generation rate.
3. The values of Ns near the plates are more than they are at the interface, indicating that friction due to surface on the fluids increases entropy generation rate.
4. The values of Ns in zone-I are more than they are in the zone-II near the plates. This indicates the more is the viscosity of the fluid, the more is the entropy generation rate.

5. The Bejan number is maximum and irreversibility ratio $\phi$ is minimum at the interface of the channel. This indicates that the amount of exergy (available energy) is maximum and irreversibility is minimum at the interface.
6. The maximum entropy generation rate shifts to each plate as viscous effects become more important since the plates act as strong irreversibility producers due to more fluid frictions in plate regions.
7. As the slip parameter increases, entropy generation rate increases.

## REFERENCES


[1] Bejan A., A study of entropy generation in fundamental convective heat transfer, *Journal of Heat Transfer.,* Vol. 101(4), 1979, pp. 718-725.

[2] Bejan A., Second law analysis in heat transfer, *Energy,* Vol. 5, 1980, pp. 720-732.

[3] Bejan A., Entropy Generation Minimization, CRC Press, Boca Raton, New York, 1996.

[4] Bejan A., Entropy minimization: the new thermodynamics of finite-size devices and finite-time processes, *Journal of Applied Physics.,* Vol. 79(3), 1996, pp. 1191-1218.

[5] Chaturani P., and Samy R P., A study of non-Newtonian aspects of blood flow through stenosed arteries and its applications in arterial diseases, *Biorheology,* Vol. 22(6), 1985, pp. 521–531.

[6] Bird R.B., Stewart W.E., and Lightfoot E.N., Transport phenomena, John Wiley and Sons, Inc, New York, 1960.

[7] Ramchandra Rao A., and Srinivasan Usha., Peristaltic transport of two immiscible viscous fluids in a circular tube, *Journal of Fluid Mechanics,* Vol. 298, 1995, pp. 271–285.

[8] Bhattacharya R. N., The flow of immiscible fluids between rigid plates with a time dependent pressure gradient. *Bulletin of the Calcutta Mathematical Society,* Vol. 1, 1968, pp. 129–137.

[9] Kapur J.N., and Shukla J.B., The flow of incompressible immiscible fluids between two parallel plates, *Applied Scientific Research,* Vol. 13, 1962.

[10] Bakhtiyarov, S, I., and Siginer D A., A note on the laminar core-annular flow of two immiscible fluids in a horizontal tube. *Proceed. Int. Symposium on liquid-liquid two phase flow and transport phenomena,* Begell house, Inc. Santa Barbara, pp. 107–111, 1997.

[11] Chamkha Ali J., Flow of two immiscible fluids in porous and nonporous channels, *Journal of Fluids Engineering,* Vol. 122(1), 2000, pp. 117–124.

[12] Vajravelu K., Arunachalm P.V., and Sreenadh S., Unsteady flow of two immiscible conducting fluids between two permeable beds, *Journal of Mathematical Analysis and Applications*, Vol. 196(3), 1995, pp. 1105–1116.

[13] Vijayakumar Varma S., and Syam Babu M., A Brinkman model for MHD viscous incompressible flow through porous channel, *Indian Journal of Pure Applied Mathematics*, Vol. 16(7), 1985, pp. 796–806.

[14] Iyengar T. K.V., and Punnamchandar Bitla., Pulsating flow of an incompressible couple stress fluid between permeable beds, *World Academy of Science, Engineering and Technology,* Vol. 80, 2011, pp. 1355–1365.

[15] Waqar A. Khan., and Gorla R.S.R., Second Law Analysis For mixed convection in non-Newtonian fluids over a horizontal plate embedded in a porous medium, *Special Topics and Reviews in Porous Media,* Vol. 1(4), 2010, pp. 353–359.

[16] Hooman K., and Ejlali, A., Entropy generation for forced convection in a porous saturated circular tube with uniform wall temperature, *International Communications in Heat and Mass Transfer,* Vol. 34(4), 2007, pp. 408–419.

[17] Tamayol A., Hooman k., and Bahrami M., Thermal analysis of flow in a porous medium over a permeable stretching wall, *Transport in Porous Media,* Vol. 85(3), 2010, pp. 661–676.

[18] Morosuk T.V., Entropy generation in conduits filled with porous medium totally and partially, *International Journal of Heat and Mass Transfer,* Vol. 48, 2005, pp. 2548–2560.

[19] Mahmud S., and Fraser R.A., Magnetohydrodynamic free convection and entropy generation in a square porous cavity, *International Journal of Heat and Mass Transfer*, Vol. 47, 2004, pp. 3245–3256.

[20] Mahmud S., and Fraser R.A., Mixed convection radiation interaction in a vertical porous channel: Entropy generation, *Energy,* Vol. 28(15), 2003, pp. 1557–1577.

[21] Tasnim S.H., Mahmud S., and Mamun M.A.H., Entropy generation in a porous channel with hydro magnetic effect, *Exergy: An International Journal*, Vol. 2(4), 2002, pp. 300–308.

[22] Kamel Hooman., Second law analysis of thermally developing forced convection in a porous medium, *Heat Transfer Research,* Vol. 36(6), 2005, pp. 437–448.

[23] Chauhan D. S., Vikas Kumar., Effects of slip conditions on forced convection and entropy generation in a circular channel occupied by a highly porous medium: Darcy extended Brinkman-Forchheimer model, *Turkish Journal of Engineering and Environmental Sciences,* Vol. 33, 2009, pp. 91–104.

[24] Paresh Vyas., Archana Rai., Entropy regime for radiative MHD Couette flow inside a channel with naturally permeable base, *International Journal of Energy and Technology,* Vol. 5(19), 2013, pp. 1–9.

[25] Kamisli F., and Oztop H.F., Second law analysis of the 2D laminar flow of two-immiscible, incompressible viscous fluids in a channel, *Heat and Mass Transfer,* Vol. 44(6), 2008, pp. 751–761.

[26] Ramana Murthy J. V., and Srinivas J., Second law analysis for the Poiseuille flow of immiscible micropolar fluids in a channel, *International Journal of Heat and Mass Transfer*, Vol. 65, 2013, pp. 254–264.

[27] Stokes V. K., Couple stresses in fluids, *The Physics of Fluids*, Vol. 9(9), 1966, pp. 1709–1715.

[28] Stokes V. K., Theories of Fluids with Microstructures. Springer, New York, 1984.

[29] Ariman T., and Cakmak A.S., Couple stresses in fluids, *The Physics of Fluids,* Vol. 10, 1967, pp. 2497–2499.

[30] Mekheimer K. S., Peristaltic transport of a couple stress fluid in a uniform and non-uniform channels, *Biorheology,* Vol. 39(6), 2002, pp. 755–765.

[31] Srivastava L.M., Peristaltic transport of a couple stress fluid, *Rheologica Acta*, Vol. 25(6), pp. 638–641, 1986.

[32] Beavers G.S., Joseph D.D., Boundary conditions at a naturally permeable wall, *Journal of Fluid Mechanics*, Vol. 30(1), 1967, pp. 197–207.

[33] Darcy H., Les fontaines publiques de la ville de Dijon, Victor Darmon Paris, 1856.

[34] Brinkman H.C., A calculation of the viscous force exerted by a flowing fluid on a dense swarm of particles, *Applied Scientific Research,* Vol. 1(1), 1949, pp. 27–34.

[35] Nield D. A., The Beavers-Joseph boundary condition and related matters: A historical and critical note, *Transport in Porous Media,* Vol. 78, 2009, pp. 537–540.

[36] Bejan A., Second law analysis in heat transfer and thermal design, *Advances in Heat Transfer,* Vol. 15, 1982, pp. 1-58.

[37] Paoletti S., Rispoli F., and Sciubba E., Calculation exergetic loses in compact heat exchanger passages, *ASME AES*, Vol. 10(2), 1989, pp 21–29.